Electronic Supplementary Information

LAMP-generated H^+ ions-induced dimer i-motif as signal transducer for ultrasensitive electrochemical detection of DNA

Xiaoyu Hua, Enfen Yang, Wenting Yang, Ruo Yuan* and Wenju Xu*

Key Laboratory of Luminescent and Real-Time Analytical Chemistry (Southwest University), Ministry of Education, School of Chemistry and Chemical Engineering, Southwest University, Chongqing 400715, PR China

*Corresponding authors: Tel.: +86 23 68252277; Fax: +86 23 68253172.

E-mail address: xwju@swu.edu.cn (W. J. Xu), yuanruo@swu.edu.cn (R. Yuan).

Table of contents

Experimental section

Reagents and chemicals. Bacillus stearothermophilus (Bst) DNA polymerase and 100 mM $MgSO_4$ were obtained by New England Biolabs Ltd. (Beijing, China). Chloroauric acid ($HAuCl_4 \cdot 4H_2O$), bovine serum albumin (BSA) and 6-mercaptohexanol (MCH) were purchased from Sigma-Aldrich (St. Louis, MO, USA). Betaine, thrombin (TB), immunoglobulin G (IgG), exonuclease III (ExoIII) and deoxynucleotide triphosphates (dNTPs) were provided by Sangon Biotech Co. Ltd (Shanghai, China). They also provided us oligonucleotides used in this work: Flu A virus biomarker DNA (fDNA) screened and cloned into pUC57 plasmid,[1] six primers (FIP, BIP, F3, B3, LF and LB) and all other oligonucleotides, which were purified by high-performance liquid chromatography. Tris (hydroxymethyl) aminomethane hydrochloride (Tris-HCl, pH 7.4) contained 140 mM NaCl, 5 mM KCl, 1 mM $CaCl_2$ and 1 mM $MgCl_2$ provided by Roche (Switzerland). Phosphate buffered saline (PBS, pH 7.0) was used as the working solution. Deionized (DI) water (Milli-Q, Millipore, 18.2 MΩ·cm) was used in our total experiments. The detailed base sequences of all oligonucleotides were listed in Table S1.

Table S1 Oligonucleotides sequences used in this work

Name	Sequence (5' to 3')
Flu A virus biomarker DNA (fDNA)	GCGCTCATGGAATGGCTAA(**F3**)AGACAAGACCAATCC TGTCACCTCTGA(**F2**)CTAAGGGGATTTTAGGATTTGTG TTCACGCTCACCGTGCC(**F1**)CAGTGAGCGAGGACTGC AGCGTAG(**B1c**)ACGCTTTGTCCAAAATGCCCTTAATGG GAATGGGGATCCAAAC(**B2c**)AACATGGACAGAGCGGT CA(**B3c**)

Forward inner primer FIP (F1c-F2)	GGCACGGTGAGCGTGAACAC(**F1c**)-TTTT-ACCAATCCTGTCACCTCTGA(**F2**)
Backward inner primer BIP (B1c-B2)	GAGCGAGGACTGCAGCGTAG(**B1c**)-TTTT-GTTTGGATCCCCATTCCCAT(**B2**)
Forward out primer (F3)	GCGCTCATGGAATGGCTAA
Backward out primer (B3)	TGACCGCTCTGTCCATGTT
Loop primer (LF)	AAATCCTAAAATCCCC
Loop primer (LB)	CGCTTTGTCCAAAATGCC
Affinity strand 1 (AS1)	TTGCTGTCACCAAAAA*CCCTAACCC*
Affinity strand 2 (AS2)	*CCCTAACCC*TTTTAATGAATCCACGT
Protection strand (PS)	**ACGTGGATTCAGTGACA**GCAAC
DNA walker (**W**)	NH_2-T_n-CCCC**TGTCACTGAATCCACGT**CCCTCCTGTTTT
Hairpin signal probe (Fc-SP)	NH_2-$(CH_2)_6$-CGTCCCTCCTCGTTTTTATTTTTTTTTTGCAGGAGGGACGTGGAT-Fc
Hairpin signal probe (Fc-SP')	NH_2-$(CH_2)_6$-CGTCCCTCCTCGTTTTTATTTTTTTTTTGCAGGAGGGACGTGGAT
$AS1_{BHQ1}$	TTGCTGTCACCAAAAACCCTAACCC-BHQ1
$AS2_{FAM}$	FAM-CCCTAACCCTTTTAATGAATCCACGT
Nosema bombycis gene DNA (PTP1)	CTACTGGATCAGGTGTTCCTTGTATTCCAGTATCTTCAACCGGTGGCCATCCAAGTAATCTCGTTGGCGGTGGTTTCCCAAGTAATGCACAAGTCACTCAAGCCCCATGTGTCCCATCACAAGCTCATCATCCAGTAGCAAGTGTTCCAGTAACGAGTGTCCCAGTAAATGCTGTTCCAATGACCAGTGCCCCTGTTACACCACTTGGCCCTTCTTATTACGGATCTTCAAGCCTTCCACCATCAGGCTCTCATCCTACTGCTCCTTGTTGT

*n = 10, 20, 30, 40, 50 and 60.

The target fDNA, the template of LAMP consisted of six distinct regions: F1, F2, F3, B1c, B2c and B3c, which are specifically interacted with forward/backward inner primers (FIP, F1c-F2; and BIP, B1c-B2) and outer primers (F3 and B3). Especially, two loop primers (LF and LB) are designed to accelerate LAMP reaction.[2] In two affinity strands (AS1 and AS2), the C-rich sequences (CCCTAACCC, designated as italicized letters) are capable of being folded into DiMS at slight acid condition, and the underlined bases are cooperatively complementary to those of a protection strand (PS). Especially, the bolded bases of PS are complementary to those of a NH_2-labeled DNA walker (**W**) containing a thymine-rich spacer (T_n, n=10, 20, 30, 40, 50 and 60) as a flexible linker. Importantly, the double underlined bases of **W** are complementary to those of the hairpin signal probe dually ended with NH_2 and redox active ferrocene (Fc-SP). To minimize the interference of Fc signals, Fc-SP' with the same sequence as Fc-SP and without Fc labeling was used to investigate CV and EIS response in $[Fe(CN)_6]^{4-/3-}$ (pH 7.0). Especially, black-hole quencher (BHQ1)-labeled $AS1_{BHQ1}$ and fluorophore FAM-labeled $AS2_{FAM}$ were designed and used to construct DiMS for investigating the pH-dependence and stability of DiMS at different pH. The base sequence of $AS1_{BHQ1}$ and $AS2_{FAM}$ were the same as AS1 and AS2. PTP1 as an interferent was used to verify the specificity of our biosensor.

LAMP reaction and DiMS assembly. LAMP reaction and DiMS assembly were easily carried out. Briefly according to previous methods,[2,3] 5 μL fDNA with different concentrations was added in a 35 μL solution containing each 0.4 μM of F3 and B3, each 2.0 μM of FIP and BIP, each 0.8 μM of LF and LB, 1.0 M betaine, 14 U Bst, 6

mM $MgSO_4$, 6 mM NH_4Cl, 1 mg mL^{-1} BSA, 0.1% Triton-X 100, and 2.8 mM dNTPs. After kept at 65 ^oC for 45 min to perform LAMP reaction, the resultant mixture was heated to 95 ^oC for 5 min. When cooling down to room temperature (RT), 1 μL of each AS1 (20 μM) and AS2 (20 μM) was introduced into the solution containing LAMP-H^+, allowing for the assembly of DiMS through semi-protonated C·CH^+ pairs and four pairs of hybridized A-T bases between AS1 and AS2.[4] Only in this case, the unpaired 5' end of AS1 together with the unpaired 3' end of AS2 overhung in DiMS can hybridize with PS.

Fabrication of the biosensor. After pretreated by polishing with 0.3 and 0.05 μm Al_2O_3 powder and sonicating in anhydrous ethanol and DI water, a clean GCE was electrodeposited in $HAuCl_4$ (1%) at –0.2 V constant potential for 40 s. Then 10 μL Fc-SP (2 μM) and 10 μL of a double strand (**W**:PS) hybridized by PS (0.2 μM) and **W** (0.2 μM) were incubated at RT for 16 h. After adding 6-mercaptohexanol (MCH) (0.1 mM) as blocking agent for 10 min, 10 μL of the as-assembled DiMS was introduced, allowing for the hybridization of DiMS with PS. Within 3 h, **W** was released and simultaneously Fc-SP was unfolded. When incubating 10 μL ExoIII (10 U) in the resultant electrode surface, the unfolded Fc-SP was cleaved by ExoIII within 2 h at 37 ^oC, releasing **W** again for continuous unfolding and ExoIII-assisted cleavage of other Fc-SP hairpins. Of note, after each step of operation, the resultant electrode was gently washed with Tris (hydroxymethyl) aminomethane hydrochloride (Tris-HCl, pH 7.4) to remove the supernatant species from the electrode surface. As such, all the cleaved segments with Fc in the final step were washed off, minimizing the false

positive signal. Finally, the obtained electrode was directly measured in $[Fe(CN)_6]^{4-/3-}$ (pH 7.0) or PBS (pH 7.0) to investigate CV/EIS or SWV signals.

Apparatus. Square wave voltammetry (SWV), cyclic voltammetry (CV) and Electrochemical impedance spectroscopy (EIS) were performed on a CHI 760E electrochemistry workstation (Shanghai Chenhua Instruments Co., Ltd., China) containing a conventional three-electrode system with a glassy carbon electrode (GCE, in 4 mm diameter) as the working electrode, a saturated calomel electrode (SCE) as the reference electrode, and a platinum wire as the auxiliary electrode. DiMS was characterized by using circular dichroism (CD) spectrum (CHIRASCAN CD, Applied Photophysics Ltd, UK) measured in the range of 220-320 nm and UV-visible (UV-Vis) spectrum (UV-2501 PC Spectrometer, Shimadzu, Japan) recorded in 220-340 nm range. Polyacrylamide gel electrophoresis (PAGE) was carried out by a DYY-8C electrophoretic apparatus (Beijing, Wo De Life Sciences Instrument Co., Ltd., China), and the gel images were taken by a Bio-Rad imaging system (Hercules, CA, USA). LAMP reaction was performed in a heating incubator (Shanghai Boxun Industry & Commerce Co., Ltd, China). The pH value after LAMP reaction was monitored by a micro pH electrode (PHR-146B, LAZAR Research Laboratories, Inc. Los Angeles, CA) connected in a pH meter (PHS-3C, Shanghai INESA & Scientific Instrument C., Ltd., China). Atomic force microscope (AFM) images were performed in Zhongkebaice Technology Service Co., Ltd. Beijing, China. The average hydrodynamic diameters were obtained by the dynamic laser light scattering (DLS, ZEN3600, Malvern).

Electrochemical measurements. CV response was measured in 0.1 M PBS (pH 7.0) containing 5 mM $[Fe(CN)_6]^{4-/3-}$ (pH 7.0) under –0.2–0.6 V potential range with a scan rate of 100 mV s^{-1}. Electrochemical impedance spectroscopy (EIS) was measured in 0.1 M PBS (pH 7.0) containing 5 mM $[Fe(CN)_6]^{4-/3-}$ (pH 7.0) in the acfrequency range of 10^{-1} to 10^5 Hz with an excitation signal of 5 mV and formal potential of 220 mV. SWV signal was recorded in phosphate buffered saline (PBS, pH 7.0) in the potential range of 0.3 to 0.55 V with a frequency of 15 Hz, and the peak current *I* (μA) of SWV corresponding to around +0.45 V was used to investigate the performance of this biosensor. In our experiments, the working solution PBS (pH 7.0) contained 10 mM Na_2HPO_4, 10 mM KH_2PO_4 and 2 mM $MgCl_2$.

Polyacrylamide gel electrophoresis. 8% non-denaturing polyacrylamide gel (PAGE) was used to to demonstrate the DNA reaction in this work. The DNA samples and the DNA loading buffer were mixed at a volume ratio of 5:1, and the electrophoresis was conducted at 1 × TBE buffer (pH 8.0 and 6.5). Followed by stained with ethidium bromide for 20 min, then the gel images were taken under the UV light illumination.

Results and discussion

The generation of H^+ during LAMP reaction.

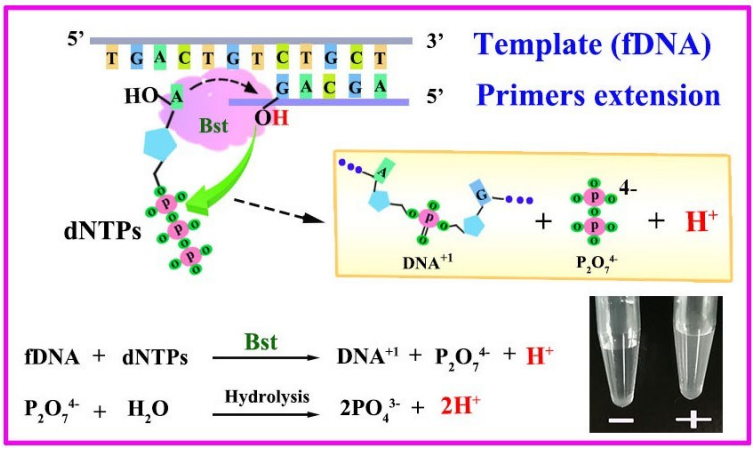

Scheme S1 Schematic diagram of LAMP-generated H^+ ions using Flu A virus biomarker DNA (fDNA) as template. With the help of dNTPs and Bst, 3'-hydroxy group (-OH) of the growing DNA strand (DNA^{+1}) would have a nucleophilic attack on α-phosphate group of incoming dNTPs. As a result, a newly formed nucleotide base would replace a proton and release a pyrophosphate ($P_2O_7^{4-}$) that was further hydrolyzed to produce two H^+ ions. Inset: the picture of two solutions after LAMP reaction without (-) and with (+) fDNA (100 ng μL^{-1}).

Working principle of LAMP reaction.

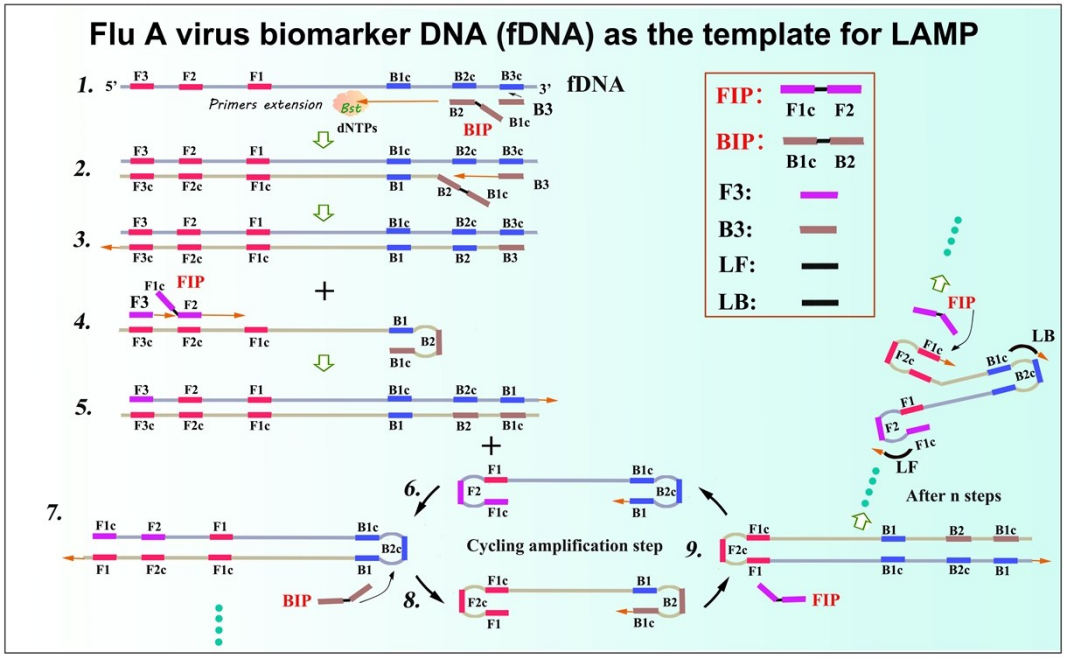

Scheme S2 Schematic diagram of the LAMP mechanism, Flu A virus biomarker DNA (fDNA) as the template. With the help of Bst, dNTPs, and all the primers (FIP, BIP, F3, B3), the dumbbell-

like DNA form (structure 6) is generated. Then, in cycling amplification step, DNAs of this form are generated continuously. Loop primers (LF and LB) are used to accelerate the reaction.

Atomic force microscopy. Compared with regular DNA, i-motif structure has a closer stacking of bases due to the specific geometry conformation.[5,6] As shown in Fig. S1, the AFM images showed that the DiMS being deposited on mica adopted unusual spherical shapes, which ascribed to the compact structure of dimer i-motif. And the number of bright spherical dots was increased due to the formation of more DiMS at decreased pH. Hence, these observations would verify that the formation of DiMS was releated to the amount of H^+.

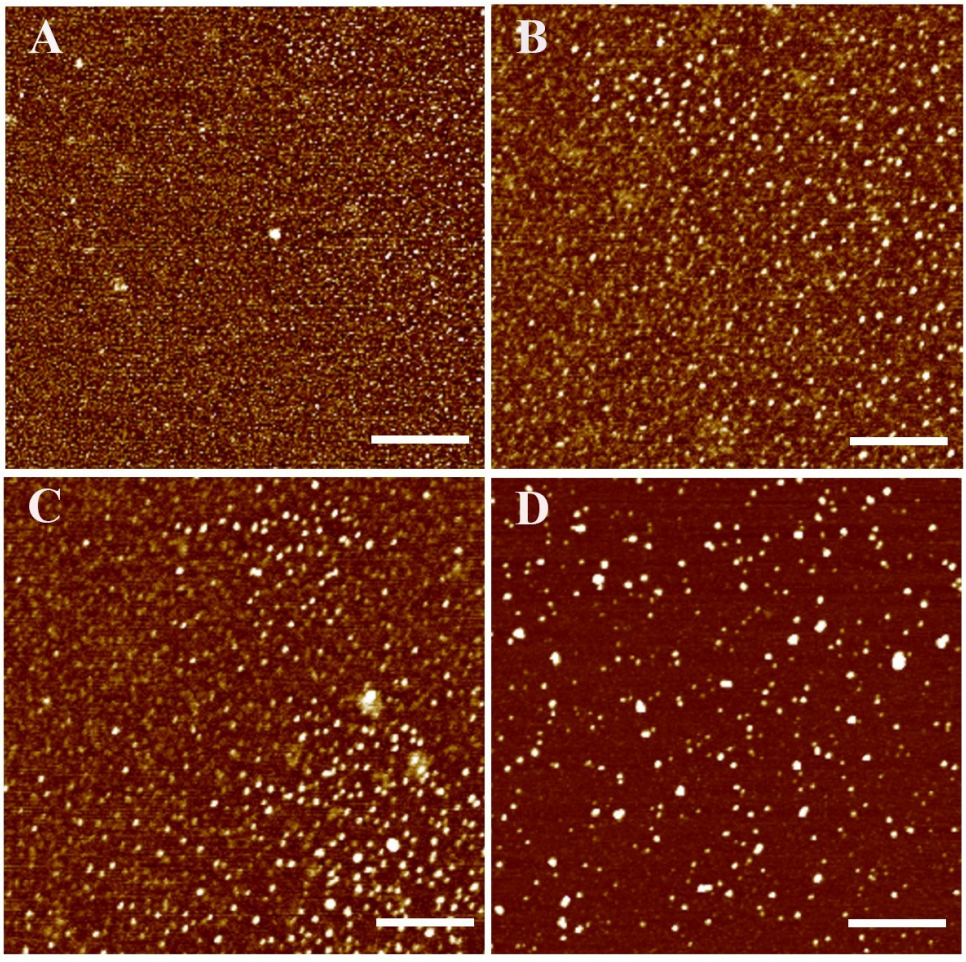

Fig. S1 AFM images of DiMS formed at different pH: (A) pH 6.8, (B) pH 6.4, (C) pH 6.0 and (D)

pH 5.6. The concentration of both AS1 and AS2 was 500 nM. The scale bars are 200 nm.

Dependent releationship between DiMS and H^+. In order to further demonstrate the proportional relationship between DiMS and LAMP-H^+, we utilized fluorescent method to approximately evaluate DiMS formation *vs*. changed pH in Tris-HCl buffer. Especially, we used $AS1_{BHQ1}$ and $AS2_{FAM}$ to construct DiMS at different pH. Significantly, the formation of DiMS brought FAM approaching to BHQ1 closely, resulting in the fluorescence quenching of FAM. From Fig. S2A, with the decrease of buffer pH in the range of 8.0 to 4.0, the fluorescence emission of the formed DiMS (excited at 497 nm) gradually decreased.[7] Fig. S2B listed the resultant fluorescence intensity (*F*) collected at 520 nm *vs*. changed pH. Obviously, the corresponding *F* was good proportional to pH in the range of 7.0-4.6 (Fig. S2C). On the other hand, it was reported that LAMP-H^+ was dose-dependent on the targeted DNA as LAMP template, and generally pH variation in LAMP was 0-1.5.[8,9] Thus, these observations would further verify the dependent relationship between DiMS and LAMP-H^+.

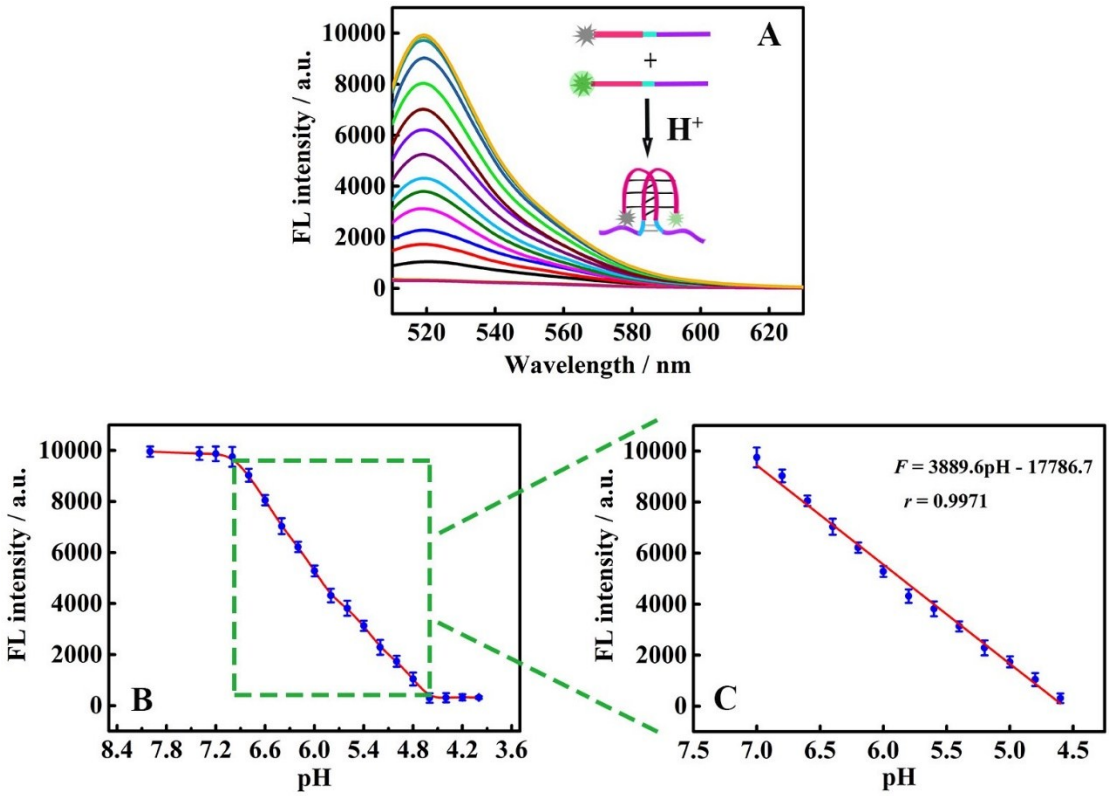

Fig. S2 (A) pH-dependent fluorescence emission spectra of DiMS in Tris-HCl buffer (pH 8.0 to 4.0); (B) The resultant relationship plotted by the corresponding fluorescence intensity (*F*) *vs*. the buffer pH from 8.0 to 4.0; (C) The resultant linear relationship of *F* vs. pH in the range of 7.0-4.6. FAM was excited at 497 nm. The concentration of both $AS1_{BHQ1}$ and $AS2_{FAM}$ was 500 nM. Error bars: standard deviation (*s*), *n*=5.

Experimental condition optimization. To achieve the optimum analytical performances, we optimized different experimental parameters, involving the electrolyte (NH_4^+) content in LAMP reaction, T numbers of T_n linker in **W**, the ratio of Fc-SP and PS, and the ExoIII-cleaved reaction time. To minimize the effect of background solution on the pH after LAMP,[8,10] a relatively weak buffering environment was crucial for the stable assembly of DiMS driven by LAMP-H^+.[11] So, NH_4Cl was chosen as the background buffer to carry out fDNA-templated LAMP

reaction, and the concentration of NH_4Cl would influence the LAMP-H^+ variation. We firstly investigated the H^+ change (-ΔpH) after and before LAMP with different concentrations of NH_4Cl ranging from 1 mM to 4 mM, and the results are shown in Fig. S3A. As could be seen, when NH_4Cl rising up to 4 mM, -ΔpH slowly increased and then rapidly increased corresponding to NH_4Cl from 5 mM to 7 mM. In the next experiments, 6 mM NH4Cl was selected as the background buffer of LAMP to minimize the hydrolysis effect of excessive NH_4^+, while maintaining the amplification efficiency and specificity.

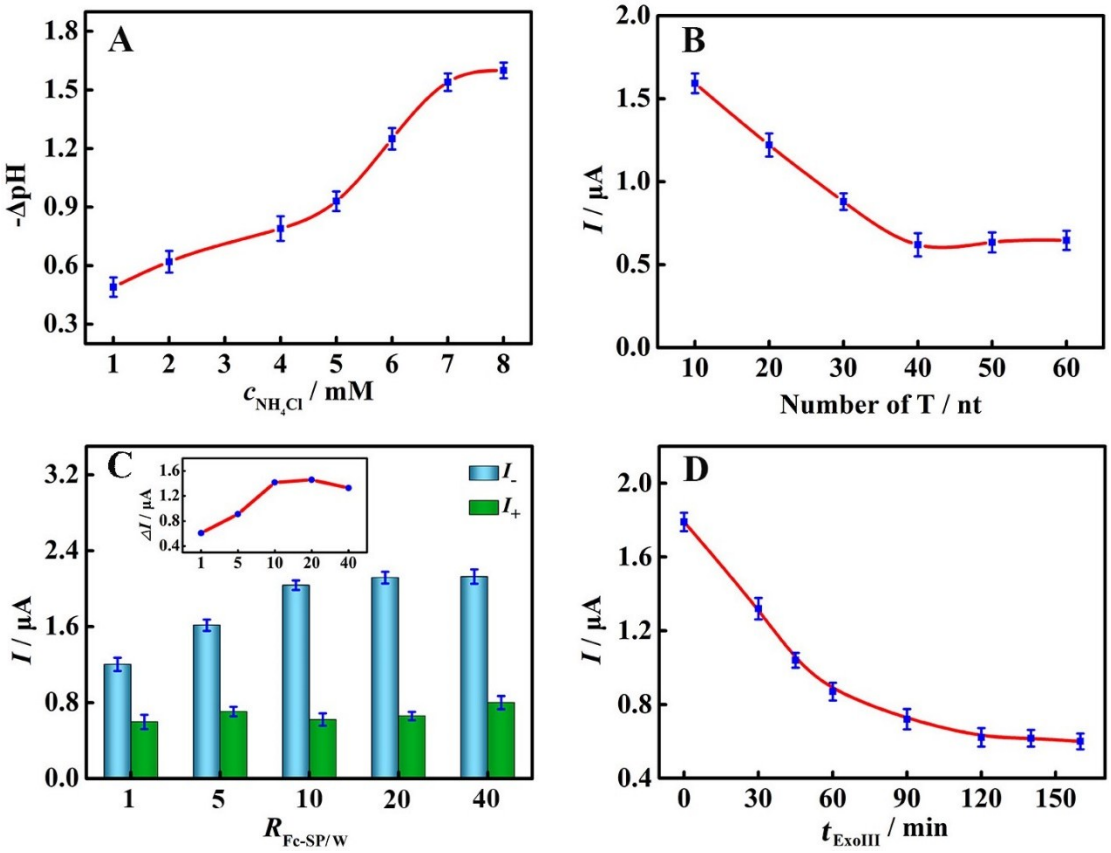

Fig. S3 Investigation of optimum experimental conditions: (A) pH variation of fDNA-templated LAMP reaction using different concentrations of NH_4Cl as background buffer; (B) SWV response to different numbers of T_n (10, 20, 30, 40, 50 and 60) tethered in **W**; (C) SWV response to different ratios of Fc-SP and **W** ($R_{Fc\text{-}SP/W}$) immobilized in the electrode surface, and in the inset

$\Delta I=I_{-}-I_{+}$ corresponding to the difference of SWV peak currents in the absence (I_{-}) or presence (I_{+}) of fDNA; (D) SWV response to different incubation time of ExoIII from 60 to 160 min. The concentrations of fDNA and ExoIII were 1 ng μL^{-1} and 10 U, respectively. Error bars: standard deviation (*s*), *n*=5.

In the modified electrode surface, the flexible T_n linker of **W** can facilitate the movement of **W** to unfold Fc-SP hairpins. The accessibility and flexibility was demonstrated by investigating the SWV response with different T numbers (T_n, n=10, 20, 30, 40, 50 and 60) tethered in **W**. From Fig. S3B, the SWV current gradually decreased with increased T numbers from 10 to 40 and leveled off at T_{40}. This may be attributed to such a fact that longer T_n linker than 40 would lower the flexibility of **W** movement and bring larger steric hindrance, which might greatly limit the efficient movement of **W** to open Fc-SP hairpins. So, the **W** with a T_{40} linker was used for our electrochemical biosensor.

The suitable ratio of Fc-SP and **W** ($R_{\text{Fc-SP/W}}$) introduced in the modified electrode surface was desired for the optimum detection sensitivity. Lower or higher ratio may cause incomplete hybridization reaction and intrinsic steric hindrance.[12] The SWV peak current of the biosensor with different ratios of $R_{\text{Fc-SP/W}}$ from 1 to 40 is shown in Fig. S3C, and in the inset, $\Delta I=I_{-}-I_{+}$ corresponded to the difference between the SWV currents in the absence (I_{-}) or presence (I_{+}) of fDNA. Apparently, the most significant signal variation was obtained for the ratio of 10 for Fc-SP and **W**.

In the biosensor construction, the final introduction of ExoIII was to drive the fast unfolding of Fc-SP hairpins and **W** walking through the successive cleavage reaction,

in which the incubation time of ExoIII (10 U) was crucial. Obviously from Fig. S3D, the SWV peak current gradually decreased and reached to the minimum at 120 min, indicating that 120 min was sufficient for the complete unfolding and ExoIII-assisted cleavage of Fc-SP hairpins in the electrode surface.

Table S2 Comparison of analytical performance of different detection methodologies for different targets

Methods	Strategies	Targets	Linear range	LOD	Ref.
Colorimetry	Target-guided deposition of silver on monodispersed Au NBPs	H5N1	1 fg μL^{-1}-2.5 pg μL^{-1}	1.0 fg μL^{-1}	13
SERS	SERS-based immunoassay with digital microfluidics	H5N1	0.5 pg μL^{-1}-5 pg μL^{-1}	74 fg μL^{-1}	14
Turbidimetry	Multiplex microfluidic LAMP system	H1N1	100 fg μL^{-1}-1 ng μL^{-1}	33.2 fg μL^{-1}	15
Colorimetry	Enzyme-induced metallization and enzyme-linked immunosorbent	H9N2	0.02 pg μL^{-1}-1pg μL^{-1}	17.5 fg μL^{-1}	16
pH meter	pH meter-combined LAMP	PTP1	0.5 pg μL^{-1}-50 ng μL^{-1}	0.17 pg μL^{-1}	8
CV	Tracing phosphate ions generated during LAMP	PTP1	50 fg μL^{-1}-50 ng μL^{-1}	17 fg μL^{-1}	17

PEC	CdSeTe@CdS:Mn core-shell quantum dots-sensitized and CuS nanocrystals conjugated signal antibodies	CEA	0.5 fg μL^{-1}-100 pg μL^{-1}	0.16 fg μL^{-1}	18
Colorimetry	Magnetic bead-based enzyme-chromogenic substrate system and cascade reaction for enzymatic formation	PSA	1 fg μL^{-1} to 30 pg μL^{-1}	0.5 fg μL^{-1}	19
Fluorometry	ExoIII-assisted target recycling amplification and DNA walker	CEA	10 fg μL^{-1}-100 pg μL^{-1}	1.2 fg μL^{-1}	20
SWV	LAMP-H^+-induced DiMS coupled with ExoIII-assisted DNA walking	Flu A	0.1fg μL^{-1}-100 ng μL^{-1}	0.018 fg μL^{-1}	Our work

SERS: surface enhanced Raman scattering. Avian influenza virus: H5N1, H1N1 and H9N2. PEC: Photoelectrochemical. CEA: carcinoembryonic antigen. PSA: prostate-specific antigen.

Recovery determination of fDNA in human serum samples. To verify the preliminary applicability of the biosensor, we used the standard addition method to evaluate the fDNA content in human serum samples kindly provided by Xinqiao Hospital, Army Medical University (Chongqing, China). Five standard fDNA solutions with different concentrations (0.10 to 10 ng μL^{-1}) were spiked into the diluted serum samples, which were further utilized to perform the separate LAMP reaction for the final fabrication of the biosensors. Based on the SWV peak currents measured in parallel five times in PBS (pH 7.0) and the linear equation obtained above, the fDNA in human serum samples could be quantified and the corresponding recovery of fDNA could be calculated. As shown in Table S3, the recovery was from

94% to 106% with RSD in the range of 2.9-5.2%, suggesting the preliminary practicability and reliability of our method in actual samples.

Table S3 Recovery determination of fDNA added in human serum samples with our electrochemical biosensor as working electrode (*n*=5)

Sample No.	Added/ng μL^{-1}	Found/ng μL^{-1}	Recovery/%	RSD/%
1	0.10	0.094	94.0	4.3
2	0.50	0.494	98.8	3.2
3	1.0	1.05	105	5.2
4	5.0	5.30	106	4.1
5	10	0.957	95.7	2.9

References

1 Y. Zhang, L. Zhang, J. S. Sun, Y. L. Liu, X. J. Ma, S. J. Cui, L. Y. Ma, J. Z. J. Xi and X. Y. Jiang, *Anal. Chem*., **2014**, 86, 7057-7062.

2 K. Nagamine, T. Hase and T. Notomi, *Mol. Cell. Probes*, 2002, **16**, 223-229.

3 K. Hsieh, A. S. Patterson, B. S. Ferguson, K. W. Plaxco and H. T. Soh, *Angew. Chem. Int. Ed*., 2012, **51**, 4896-4900.

4 B. Mir, I. Serrano, D. Buitrago, M. Orozco, N. Escaja and C. Gonzalez, *J. Am. Chem. Soc*., 2017, **139**, 13985-13988.

5 D. Zikich, K. Liu, L. Sagiv, D. Porath and A. Kotlyar, *Small*, 2011, **7**, 1029-1034.

6 A. D. Protopopova, V. B. Tsvetkov, A. M. Varizhuk, N. A. Barinov, V. V. Podgorsky, D. V. Klinov and G. E. Pozmogova, *Phys. Chem. Chem. Phys*., 2018, **20**, 3543-3553.

7 M. C. Xia, L. Cai, Y. Yang, S. C. Zhang and X. R. Zhang, *Anal. Chem*., 2019, **91**, 9168-9173.

8 S. B. Xie, Y. L. Yuan, Y. Song, Y. Zhuo, T. Li, Y. Q. Chai and R. Yuan, *Chem. Commun*., 2014, **50**, 15932-15935.

9 C. Toumazou, L. M. Shepherd, S. C. Reed, G. I. Chen, A. Patel, D. M. Garner, C. J. A. Wang, C. P. Ou, K. Amin-Desai, P. Athanasiou, H. Bai, I. M. Q. Brizido, B. Caldwell, D. Coomber-Alford, P. Georgiou, K. S. Jordan, J. C. Joyce, M. L. Mura, D. Morley, S. Sathyavruthan, S. Temelso, R. S. E. Thomas and L. L. Zhang, *Nature Methods*, 2013, **10**, 641-646.

10 J. M. Zhao, J. X. Gao, T. Zheng, Z. H. Yang, Y. Q. Chai, S. H. Chen, R. Yuan and W. J. Xu, *Biosens. Bioelectron*., 2018, **106**, 186-192.

11 B. Mir, I. Serrano, D. Buitrago, M. Orozco, N. Escaja and C. Gonzalez, *J. Am. Chem. Soc*., 2017, **139**, 13985-13988.

12 C. X. Zhu, M. Y. Liu, X. Y. Li, X. H. Zhang and J. H. Chen, *Chem. Commun*., 2018, **54**, 10359-10362.

13 S. H. Xu, W. J. Ouyang, P. S. Xie, Y. Lin, B. Qiu, Z. Y. Lin, G. N. Chen and L. H. Guo, *Anal. Chem*., 2017, **89**, 1617-1623.

14 Y. Wang, Q. Y. Ruan, Z. C. Lei, S. C. Lin, Z. Zhu, L. J. Zhou and C. Y. Yang, *Anal. Chem*., 2018, **90**, 5224-5231.

15 X. Fang, H. Chen, S. Yu, X. Jiang and J. Kong, *Anal. Chem*., 2011, **83**, 690-695.

16 H. F. Zhang, X. M. Ma, S. S. Hu, Y. Lin, L. H. Guo, B. Qiu, Z. Y. Lin and G. N. Chen, *Biosens. Bioelectron*., 2016, **79**, 874-880.

17 S. B. Xie, Y. L. Yuan, Y. Q. Chai and R. Yuan, *Anal. Chem*., 2015, **87**, 10268-10274.

18 G. C. Fan, H. Zhu, D. Du, J. R. Zhang., J. J. Zhu and Y. H. Lin, *Anal. Chem*., 2016, **88**, 3392-

3399.

19 W. Q. Lai, D. P. Tang, J. Y. Zhuang, G. N. Chen and H. H. Yang, *Anal. Chem*., 2014, **86**, 5061-5608.

20 M. Q. He, K. Wang, W. J. Wang, Y. L. Yu and J. H. Wang, *Anal. Chem*., 2017, **89**, 9292-9298.